International Journal of
Energy & Technology

www.journal-enertech.eu

ISSN 2035-911X

International Journal of Energy & Technology 4 (20) (2012) 1–12

MASS TRANSFER WITH CHEMICAL REACTION IN MHD MIXED CONVECTIVE FLOW ALONG A VERTICAL STRETCHING SHEET

Gurminder Singh[1], P.R. Sharma[2], A.J. Chamkha[3]

[1]Birla Institute of Technology (Ranchi), Ext. Center Jaipur, 27, Malviya Industrial Area, Jaipur-302017, India
garry_mal@yahoo.com
[2]Department of Mathematics, University of Rajasthan, Jaipur - 302055, India
profprsharma@yahoo.com
[3]Manufacturing Engineering Department, The Public Authority for Applied Education and Training, Shuweikh, 70654, Kuwait
achamkha@yahoo.com

ABSTRACT

The aim of the paper is to investigate steady mixed convection flow in an incompressible viscous electrically conducting fluid with homogenous chemical reaction, which consumes species, along a non-conducting vertical, linearly stretching sheet in the presence of transverse magnetic field when sheet is subjected to different thermal boundary conditions i.e. either isothermal/non-isothermal or with constant heat flux. The governing equations of continuity, momentum, energy and species diffusion in the boundary layer are transformed into ordinary differential equations using similarity transformation. The resulting coupled non-linear ordinary differential equations are solved using Runge-Kutta fourth order method alongwith shooting technique. The velocity, temperature and concentration distributions are discussed numerically and presented through graphs. The numerical values of skin-friction coefficient, Nusselt number and Sherwood number at the surface are discussed numerically for various values of physical parameters and presented through Tables.

Keywords: Steady flow; MHD; mixed convection; stretching sheet; mass transfer; chemical reaction.

1. INTRODUCTION

Heat transfer when the fluid flows along the surface due to temperature difference between the surface and fluid is called convection and is studied in the class of problems called boundary layer flow of viscous fluid. If the fluid flow is affected/modified by the external force such as if fluid has its own velocity or if surface is moving/ stretching etc. the process is called as mixed convection. Now, as the fluid flow along the surface it exerts drag on the surface, which is measured in dimensionless form as skin-friction. Further as the fluid flows along the surface, due to temperature difference between surface and fluid, temperature diffuses ($T_w > T_\infty$) from surface to fluid and the heat transfer at the surface is measured in terms of Nusselt number. Similar to heat transfer, if there is concentration gradient of specie between surface and fluid the specie diffuses ($C_w > C_\infty$) from surface into the fluid and the mass transfer at the surface is measured in terms of Sherwood number. There are cases when fluid reacts with the specie and hence specie concentration is modified continuously giving rise to complex mass transfer phenomena at the surface. The fluid flow, heat and mass transfer along the surface can be modified if magnetic field perpendicular to surface i.e. transversely is applied to the surface and such flows are called Magnetohydrodynamic (MHD) flows. Thus, Magnetohydrodynamics is the study of motion of an electrically conducting incompressible fluid in the presence of magnetic field i.e. an electromagnetic field interacting with the velocity field of an electrically conducting fluid. Hydromagnetic flows are important because on application of magnetic field, the heat and mass transfer can be modified to produce desired affect on the industrial products. In many industrial applications of electrochemistry and in polymer processing the surface undergoes stretching along with chemical treatment within the fluid and therefore understanding the heat and mass transfer characteristic is must for desired quality of final product. Chambrė and Young [1] pioneered the study of chemically reacting and diffusing species in the boundary layer. Sakiadis [2] initiated the study by analyzing the boundary layer fluid flow over continuous surface. Erikson et al. [3] investigated heat and mass transfer with suction or injection on the flat plate. Crane [4] presented the flow over a stretching sheet and obtained similarity solution in closed analytical form. Chin [5] observed the mass transfer on continuously moving sheet electrode. Gupta and Gupta [6] studied the heat and mass transfer characteristic on a

stretching sheet with suction and injection. Flow and heat transfer characteristics of fluid on stretching sheet with variable surface temperature condition have been investigated by Grubka and Bobba [7]. Noor [8] studied the characteristics of heat transfer on stretching sheet. Das et al. [9] analyzed mass transfer affect on fluid flow due to impulsively started vertical plate with constant heat flux. Chamkha [10] observed three-dimensional convection on a stretching surface in the presence of heat generation of absorption. Afify [11] presented MHD free convective flow over a stretching surface with homogenously chemically reacting species being consumed in the process. Abo-Eldahab [12] extended the study presented by Chamkha [10] considering mass transfer. Ishak et al. [13,14] have studied fluid flow and heat transfer models along stretching sheet and shown presence of dual solution of which one is stable while other is a possible solution.

Motivated by the above work, aim of the paper is to investigate steady mixed convection flow in an incompressible viscous electrically conducting fluid with homogenous chemical reaction, which consumes species, along a non-conducting vertical, linearly stretching sheet in the presence of transverse magnetic field when the sheet is either isothermal/non-isothermal or subjected to a constant heat flux.

2. FORMULATION OF THE PROBLEM

Consider steady laminar mixed convective flow of a viscous incompressible electrically conducting fluid along a non-conducting, vertical sheet, which is stretched in its own plane with velocity $u_w = cx$. The fluid chemically reacts with species and consumes the species within the boundary layer. The ambient fluid far away from surface has temperature T_∞ and concentration zero. The *x*-axis is taken along the sheet and *y*-axis is normal to the plate. Magnetic field of uniform intensity B_o is applied in *y*-direction. The Physical model is shown in the Figure 1.

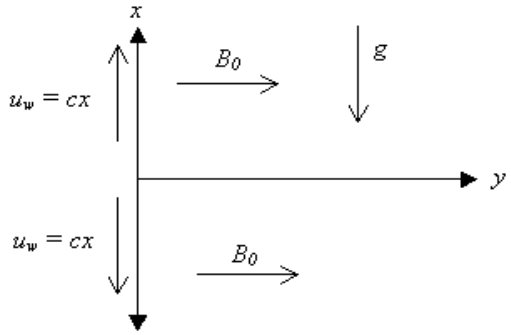

Fig. 1. Physical Model.

It is assumed that the external field is zero, also electrical field due to polarization of charges and Hall effect are neglected. Incorporating the Boussinesq's approximation within the boundary layer, the governing equations of continuity, momentum, energy and mass diffusion (Jeffery [17], Bejan [18]) respectively are given by:

$$\frac{\partial u}{\partial x}+\frac{\partial v}{\partial y}=0, \tag{1}$$

$$u\frac{\partial u}{\partial x}+v\frac{\partial u}{\partial y}=\nu\frac{\partial^2 u}{\partial y^2}+g\beta\left(T-T_\infty\right)+g\beta C-\frac{\sigma {B_o}^2}{\rho}u, \tag{2}$$

$$u\frac{\partial T}{\partial x}+v\frac{\partial T}{\partial y}=\frac{\kappa}{\rho C_p}\frac{\partial^2 T}{\partial y^2}. \tag{3}$$

$$u\frac{\partial C}{\partial x}+v\frac{\partial C}{\partial y}=D\frac{\partial^2 C}{\partial y^2}-\lambda(C)^n. \tag{4}$$

The boundary conditions (Bejan[18]) are given by

Case-1: Prescribed surface temperature (PST)

$$y=0:\ u=ax, v=0, T=T_w=T_\infty+bx^\alpha, C=C_w$$
$$y\to\infty: u\to 0, T\to T_\infty, C\to 0 \tag{5}$$

where $\alpha = 0$ implies isothermal surface, $\alpha \neq 0$ implies non-isothermal surface.

Case-2: Prescribed heat flux (PHF)

$$y=0:\ u=ax, v=0, \frac{\partial T}{\partial y}=-\frac{q_w}{\kappa}, C=C_w$$
$$y\to\infty: u\to 0, T\to T_\infty, C\to 0 \tag{6}$$

3. METHOD OF SOLUTION

Introducing the stream function $\psi(x, y)$ such that

$$u=\frac{\partial\psi}{\partial y} \text{ and } v=-\frac{\partial\psi}{\partial x} \tag{7}$$

where $\psi(x,y)=\sqrt{a\nu}\,x f(\eta)$ and the similarity variable

$$\eta=y\left(\frac{a}{\nu}\right)^{1/2}. \tag{8}$$

It is observed that the equation (1) is identically satisfied by equation (7). Substituting equation (8) into the equations (2), (3) and (4), the resulting coupled non-linear ordinary differential equations are

Case-1: PST

$$f'''+ff''-f'^2+G_{ST}\,\theta+G_M\,\phi-M^2 f'=0, \tag{9}$$
$$\theta''+\Pr\left(f\theta'-\alpha f'\theta\right)=0, \tag{10}$$

and

$$\phi''+Sc\left(f\phi'-\varepsilon\phi^n\right)=0. \tag{11}$$

The boundary conditions are reduced to

$$f(0)=0,\ f'(0)=1,\ f'(\infty)=0, \theta(0)=1,\ \theta(\infty)=0,$$
$$\phi(0)=1 \ \textit{and}\ \ \phi(\infty)=0 \tag{12}$$

Case-2: PHF

$$f'''+ff''-f'^2+G_{HF}\,\theta+G_M\,\phi-M^2 f'=0, \tag{13}$$
$$\theta''+\Pr f\,\theta'=0, \tag{14}$$

and

$$\phi'' + Sc\left(f\,\phi' - \varepsilon\,\phi^n\right) = 0\,. \tag{15}$$

The boundary conditions are reduced to

$$f(0) = 0,\ f'(0) = 1,\ f'(\infty) = 0, \theta'(0) = -1,\ \ \theta(\infty) = 0,\\ \phi(0) = 1\ \ and\ \ \phi(\infty) = 0 \tag{16}$$

The governing boundary layer equations (9), (10) and (11) with boundary conditions (12) and equations (13), (14) and (15) with boundary conditions (16) are solved using Runge-Kutta fourth order technique along with double shooting technique (Conte and Boor [20]).

4. SKIN-FRICTION COEFFICIENT

The skin-friction coefficient at the sheet surface is given by

$$C_f = 2(\mathrm{Re})^{-1/2} f''(0)\,. \tag{17}$$

5. NUSSELT NUMBER

The rate of heat transfer in terms of the Nusselt number at the sheet surface is given by

$Nu = -(\mathrm{Re})^{1/2}\theta'(0)$ for prescribed surface temperature and

$Nu = (\mathrm{Re})^{1/2}\theta(0)$ for prescribed heat flux. (18)

6. SHERWOOD NUMBER

The rate of mass transfer in terms of the Sherwood number at the sheet surface is given by

$$Sh = -(\mathrm{Re})^{1/2}\phi'(0) \tag{19}$$

7. PARTICULAR CASES

In the absence of species diffusion equation and magnetic field for non-isothermal sheet surface (i.e. α = 1) the system of equations (1), (2) and (3) reduce to those studied by Ishak et al. [19] for steady flow and the governing equations were solved using the Keller Box scheme. It is seen from Table 1 that the results obtained for $f''(0)$ and $\theta'(0)$ by present scheme are in good agreement.

The particular case of hydromagnetic three dimensional stretching surface dealt by Chamkha [10] and Abo-Eldahab [12] match with specific cases of the present paper and the results are compared in Table 2, which again verifies the correctness of the present scheme.

The system of equations (9), (10) and (11) have been studied by Afify [11] for isothermal surface (i.e. α = 0) when T_∞ = 0. Afify [11] presented numerical values of $f''(0)$, $\theta'(0)$ and $\phi'(0)$ for different values of the parameters. It is observed that these results are self-inconsistent as for Pr = 0.71, G_{ST} = 0.5, G_M = 0.5, Sc = 0.1 M = 0.1 and α = 0, $f''(0)$ has two values which can be seen in Table 3. Some other results are also compared and presented through Table 3.

Further, it is seen from Table 3 that the values of $f''(0)$ and $-\theta'(0)$ obtained by Afify [11] do not vary with the change in parameter *n*, however the figures presented by him show distinct profiles of $f'(\eta)$ and $\theta(\eta)$, which is not possible. In view of these inconsistencies, the problem on isothermal surface is also reconsidered, results are obtained and presented.

8. RESULTS AND DISCUSSION

It is seen from Table 4 that with the increase in Schmidt number the skin-friction coefficient and heat flux decrease, while the mass flux increases from surface to fluid. Physical insight in the process explains well, the interplay between these three important aspects of convective mass transfer. Comparatively, small Schmidt number implies that the fluid has high diffusion coefficient for the species and hence in steady state the concentration of the species is higher in fluid which thereby reduces the concentration gradient at the surface and so the mass flux. Further, high concentration of the species in fluid means increase in modified buoyancy force, scaled by (C/C_w), which is reflected as increase in fluid velocity in the direction of surface velocity. This in turn implies reduced relative velocity (when fluid velocity < surface velocity) between surface and fluid and therefore the fluid experiences less drag from the surface at low Schmidt number. Adding to the discussion, large fluid velocity in boundary layer implies that the heat is convected readily and hence heat flux from surface to fluid must be larger for large fluid velocity i.e. at comparatively small Schmidt number. It is observed that with the increase in the order of reaction, the mass flux at the surface reduces marginally, while the skin-friction and heat flux are practically invariant. It is noticed that with the increase in reaction rate parameter (ε) the mass flux at the surface increases. This is explained as, with the increase in ε the mass consumption of the species in the fluid increases and hence the specie concentration reduces, and thus diffusion of mass from surface to fluid increases. A marginal decrease in the skin-friction and heat flux is also observed. It is seen that with the increase in buoyancy and modified buoyancy parameters the skin-friction parameter increases with the sign change from negative to positive, which means that at high buoyancy parameter the fluid exerts drag on the sheet surface. The higher fluid velocity near surface would imply increase in heat and mass flux, which is vindicated by the increase in numerical values of $-\theta'(0)$ and $-\phi'(0)$. It is observed that with the increase in magnetic parameter, that skin-friction decreases i.e. fluid experiences more and more drag as magnetic parameter increases. The heat and mass flux at surface reduce with the increase in magnetic parameter. It is noticed that with the increase in Prandtl number, skin-friction and mass flux decrease, while the heat flux increases at the sheet surface this happens because with the increase in Prandtl number the thickness of thermal boundary layer

decreases. Prandtl number holds the analogy with Schmidt number in terms of diffusion of heat and mass in fluid, respectively. So, from the same token as discussed for Schmidt number, the interplay of skin-friction, heat and mass flux with respect to Prandtl number is understood. It is seen that with the increase in parameter α, the skin-friction decreases and heat flux increase, while mass flux decreases marginally at the sheet surface.

The effect of variation in the parameters on skin-friction and mass flux at the surface for constant heat flux has same characteristic as discussed and presented in Table 4 for prescribed surface temperature. It is seen from Table 5 that as the Schmidt number increases the skin-friction decreases, while the surface temperature and mass flux at the surface increase. Since, the fluid velocity is higher for low Schmidt number, as discussed earlier; the heat is convected readily from surface resulting in the relatively higher cooling of the surface, so surface temperature is lower for low Schmidt number. The increase in the order of reaction and reaction rate parameter practically does not vary surface temperature.

It is observed that with the increase in buoyancy and modified buoyancy parameters the surface temperature is lowered. This should occur, because higher buoyancy means higher fluid velocity, which implies more cooling of the surface. It is noticed that with the increase in magnetic parameter the surface temperature increases, while with the increase in Prandtl number the surface temperature decreases. This would happen because reduced fluid velocity would mean heat is not convected readily and hence surface temperature increases.

Table 1. Comparison of numerical values of $f''(0)$ and $\theta'(0)$ for different values of Pr and G_{ST} are compared with the results obtained by Ishak et al. [19].

	Ishak et al. [19]		Present Paper	
	$f''(0)$	$\theta'(0)$	$f''(0)$	$\theta'(0)$
Pr = 0.7, G_{ST} = 0.0	-1.00	-0.7937	-1.00	-0.79366
G_{ST} = 1.0	-0.5076	-0.8961	-0.50751	-0.89613
G_{ST} = 10.0	2.5777	-1.1724	2.57771	-1.17244
Pr = 10, G_{ST} = 0.0	-1.00	-3.7207	-1.00	-3.72067
G_{ST} = 1.0	-0.8257	-3.7486	-0.82568	-3.74856
G_{ST} = 10.0	0.6197	-3.9524	0.61966	-3.95235

Table 2. Comparison of numerical values of $f''(0)$, $-\theta'(0)$ and $-\phi'(0)$ when G_{ST} = 0.0, G_M = 0.0, ε = 0.0 and α = 0.

	Chamkha [10]		Abo-Eldahab [12]			Present Paper		
Pr = 0.7, Sc = 0.7	$f''(0)$	$-\theta'(0)$	$f''(0)$	$-\theta'(0)$	$-\phi'(0)$	$f''(0)$	$-\theta'(0)$	$-\phi'(0)$
M^2 = 0.0	-1.0018	0.45593	-0.99917	0.45392	0.45392	-1.0000	0.453916	0.453916
M^2 = 0.2	-	-	-	0.435603	0.435603	-	0.435566	0.435566
M^2 = 0.4	-	-	-	0.419444	0.419444	-	0.41937	0.41937
Pr = 7.0, Sc = 0.7	$f''(0)$	$-\theta'(0)$	$f''(0)$	$-\theta'(0)$	$-\phi'(0)$	$f''(0)$	$-\theta'(0)$	$-\phi'(0)$
M^2 = 0.0	-1.0018	1.89691	-0.99945	1.8954	0.45392	-1.0000	1.895403	0.453916
M^2 = 0.2	-	-	-	1.87455	0.435603	-	1.87454	0.435566

Table 3. Comparison of numerical values of $f''(0)$, $-\theta'(0)$ and $-\phi'(0)$ when Pr = 0.71, G_{ST} = 0.5, G_M = 0.5, Sc = 0.1 M = 0.1 and α = 0.

	Afify [11]			Present paper		
ε (n=1)	$f''(0)$	$-\theta'(0)$	$-\phi'(0)$	$f''(0)$	$-\theta'(0)$	$-\phi'(0)$
0.1	0.59225*	0.48266	0.53793	-0.32300	0.594496	0.2045134
0.5	0.52761	0.45182	0.57911	-0.351312	0.585233	0.28691
1.0	0.48503	0.42311	0.61081	-0.374806	0.577285	0.365007
n (ε =0.1)	$f''(0)$	$-\theta'(0)$	$-\phi'(0)$	$f''(0)$	$-\theta'(0)$	$-\phi'(0)$
1	0.66059*	0.36095	1.62498	-0.32300	0.594496	0.204513
2	0.66059	0.36095	0.82886	-0.318101	0.596228	0.19518
3	0.66059	0.36095	0.58823	-0.31630	0.59676	0.191008

* self inconsistent result mentioned by Afify [11].

Table 4. Numerical values of $f''(0)$, $-\theta'(0)$ and $-\phi'(0)$ for different values of parameters for PST.

	Pr = 0.71, G_{ST} = 1.0, G_M = 0.5, M = 0.5, n =1, ε = 0.1, α = 0.0				Pr = 0.71, G_{ST} = 1.0, G_M = 0.5, M = 0.5, Sc =1, ε = 0.1, α = 0.0		
Sc	$f''(0)$	$-\theta'(0)$	$-\phi'(0)$	n	$f''(0)$	$-\theta'(0)$	$-\phi'(0)$
0.5	-0.31978	0.56570	0.50754	1	-0.31978	0.56570	0.50754
1.0	-0.36073	0.55385	0.75371	2	-0.31559	0.56709	0.48765
5.0	-0.44548	0.53962	1.80433	3	-0.314232	0.56746	0.47922
ε	Pr = 0.71, G_{ST} = 1.0, G_M = 0.5, M = 0.5, Sc = 0.5, n =1, α = 0.0			G_{ST}	Pr = 0.71, G_M = 0.5, M = 0.5, Sc = 0.5, n =1, ε = 0.1, α = 0.0		
0.5	-0.34150	0.55980	0.67855	2.0	0.11944	0.60540	0.53728
1.0	-0.35907	0.55547	0.84471	5.0	1.29135	0.68475	0.59850
G_M	Pr = 0.71, G_{ST} = 1.0, M = 0.5, Sc = 0.5, n =1, ε = 0.1, α = 0.0			M	Pr = 0.71, G_{ST} = 1.0, G_M = 0.5, Sc = 0.5, n =1, ε = 0.1α = 0.0		
2.0	0.36507	0.63071	0.55744	1.0	-0.67365	0.52352	0.47609
4.0	1.18725	0.68898	0.60331	2.0	-1.66685	0.41484	0.40423
Pr	G_{ST} = 1.0, G_M = 0.5, M = 0.5, Sc = 0.5, n =1, ε = 0.1, α = 0.0			α	Pr = 0.71, G_{ST} = 1.0, G_M = 0.5, M = 0.5, Sc = 0.5, n =1,ε = 0.1		
0.1	-0.12130	0.19337	0.55855	0.0	-0.31978	0.56570	0.50734
10	-0.60633	2.37785	0.46900	1.0	-0.37993	0.92656	0.49824

Table 5. Numerical values of $f''(0)$, $\theta(0)$ and $-\phi'(0)$ for different values of parameters for PHF.

	Pr = 0.71, G_{HF} = 1.0, G_M = 0.5, M = 0.5, n =1, ε = 0.1, α = 0.0				Pr = 0.71, G_{HF} = 1.0, G_M = 0.5, M = 0.5, Sc =1, ε = 0.1, α = 0.0		
Sc	$f''(0)$	$\theta(0)$	$-\phi'(0)$	n	$f''(0)$	$\theta(0)$	$-\phi'(0)$
0.5	-0.01581	1.68338	0.52865	1	-0.01581	1.68338	0.52865
1.0	-0.04248	1.707702	0.78479	2	-0.013510	1.68087	0.50985
5.0	-0.10687	1.73544	1.85310	3	-0.01268	1.68020	0.50185
ε	Pr = 0.71, G_{HF} = 1.0, G_M = 0.5, M = 0.5, Sc = 0.5, n =1, α = 0.0			G_{HF}	Pr = 0.71, G_M = 0.5, M = 0.5, Sc = 0.5, n =1, ε = 0.1, α = 0.0		
0.5	-0.02925	1.69429	0.69387	2.0	0.57896	1.56273	0.56370
1.0	-0.04077	1.702542	0.85638	5.0	1.97741	1.38599	0.62729
G_M	Pr = 0.71, G_{HF} = 1.0, M = 0.5, Sc = 0.5, n =1, ε = 0.1, α = 0.0			M	Pr = 0.71, G_{HF} = 1.0, G_M = 0.5, Sc = 0.5, n =1, ε = 0.1α = 0.0		
2.0	0.58501	1.54803	0.56916	1.0	-0.33784	1.79004	0.50172
4.0	1.34642	1.43320	0.61011	2.0	-1.26345	2.15030	0.43598
Pr	G_{HF} = 1.0, G_M = 0.5, M = 0.5, Sc = 0.5, n =1, ε = 0.1, α = 0.0						
0.1	1.45240	3.92371	0.66857				
10	-0.72328	0.42313	0.46611				

Figures 2 to 23 and 24 to 29 present the effects of different parameters on fluid velocity, fluid temperature and species concentration in the fluid for prescribed surface temperature (PST) and heat flux (PHF), respectively. Figures 2 to 4 depict that for PST, with the increase in the Schmidt number the fluid velocity and the concentration of the species in the fluid reduce, while the fluid temperature increases. There is significant decrease in concentration boundary layer thickness when Schmidt number increases, while boundary layer thickness vary only marginally. It is seen in figure 5 that increase in order of reaction (n) causes a marginal increase in the species concentration. Its effect on fluid velocity and temperature is negligible and hence those figures have not been included. Therefore it is concluded that effect of parameter n on species consumption is not profound. Figures 6 to 8 show that fluid velocity and species concentration decrease with the increase in parameter ε, while a slight increase in the fluid temperature is observed. The reason behind is that as ε increases, the chemical reaction consumes species concentration. Thus modified buoyancy force reduces which is reflected as reduction in fluid velocity and hence fluid temperature increases. Figures 9 to 14 show that with the increase in buoyancy and modified buoyancy

parameters the fluid velocity increases, this happens because the increase in these parameters causes in increase in buoyancy forces. Adding, the higher fluid velocity ensures better convection and distribution of temperature and concentration, respectively which is seen as lowering of fluid temperature and species concentration.

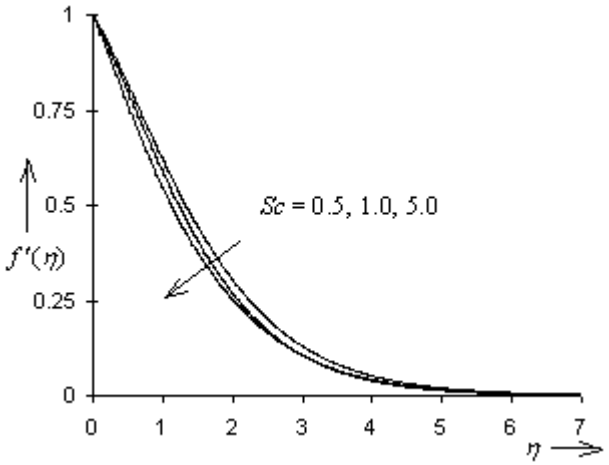

Fig. 2. Velocity distribution vs. η when Pr = 0.71, G_{ST} = 1.0, G_M = 0.5, M = 0.5, ε = 0.1, n =1 & α = 0.

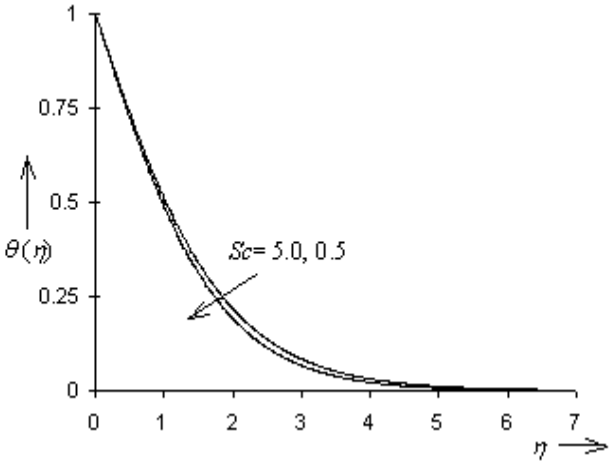

Fig. 3. Temperature distribution vs. η when Pr = 0.71, G_{ST} = 1.0, G_M = 0.5, M = 0.5, ε = 0.1, n =1 & α = 0.

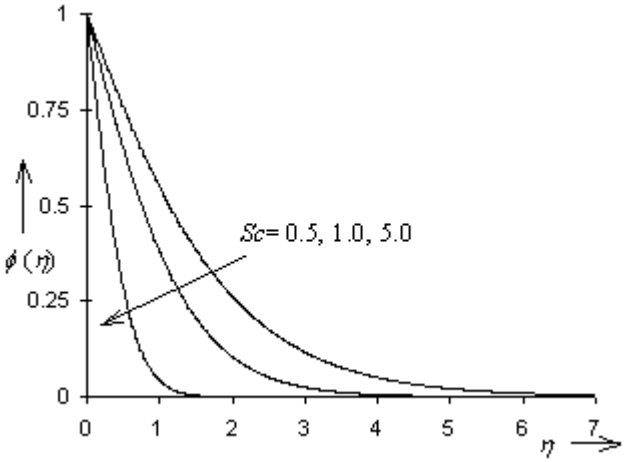

Fig. 4. Concentration distribution vs. η when Pr = 0.71, G_{ST} = 1.0, G_M = 0.5, M = 0.5, ε = 0.1, n =1 & α = 0.

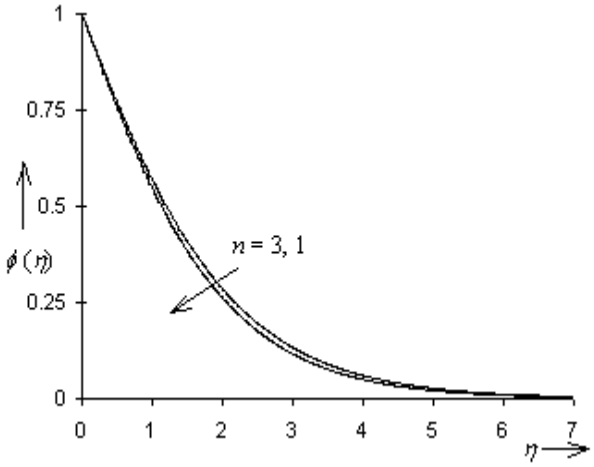

Fig. 5. Concentration distribution vs. η when Pr = 0.71, G_{ST} = 1.0, G_M = 0.5, M = 0.5, ε = 0.1, Sc =0.5 & α = 0.

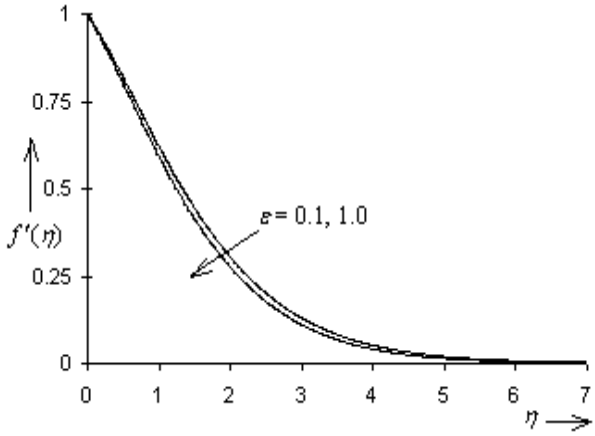

Fig. 6. Velocity distribution vs. η when Pr = 0.71, G_{ST} = 1.0, G_M = 0.5, M = 0.5, Sc = 0.

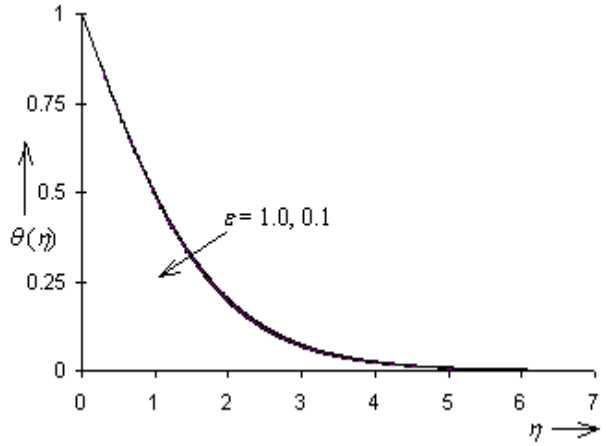

Fig. 7. Temperature distribution vs. η when Pr = 0.71, G_{ST} = 1.0, G_M = 0.5, M = 0.5, Sc = 0.5, n =1 & α = 0.

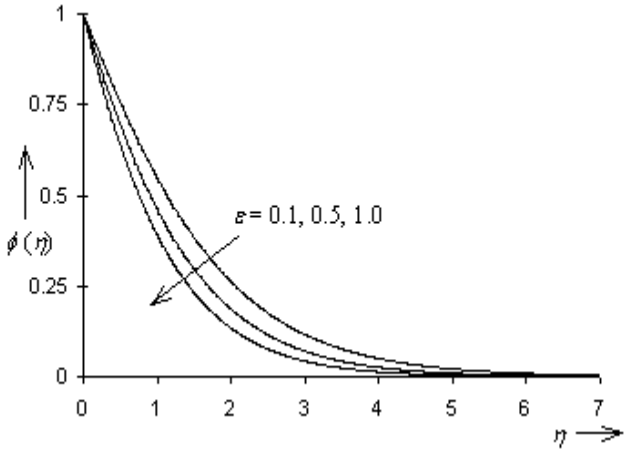

Fig. 8. Concentration distribution vs. η when Pr = 0.71, G_{ST} = 1.0, G_M = 0.5, M = 0.5, Sc = 0.5, n =1 & α = 0.

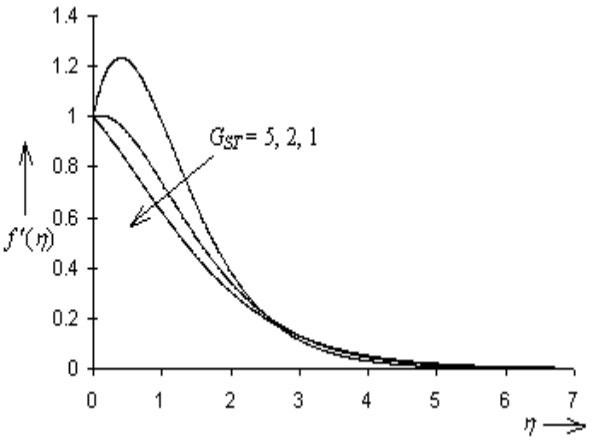

Fig. 9. Velocity distribution vs. η when Pr = 0.71, G_M = 0.5, M = 0.5, ε = 0.1, Sc = 0.5, n =1 & α = 0.

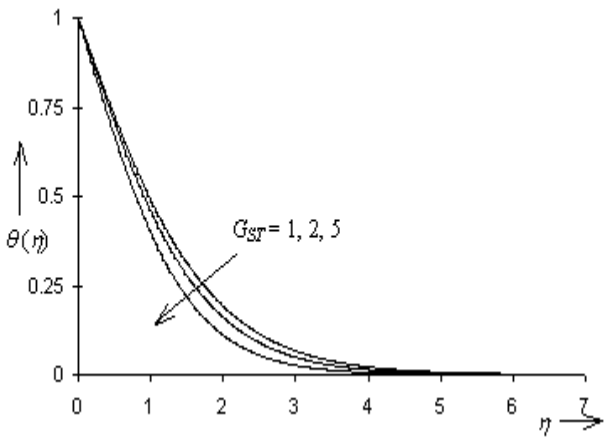

Fig. 10. Temperature distribution vs. η when Pr = 0.71, G_M = 0.5, M = 0.5, ε = 0.1, Sc = 0.5, n =1 & α = 0.

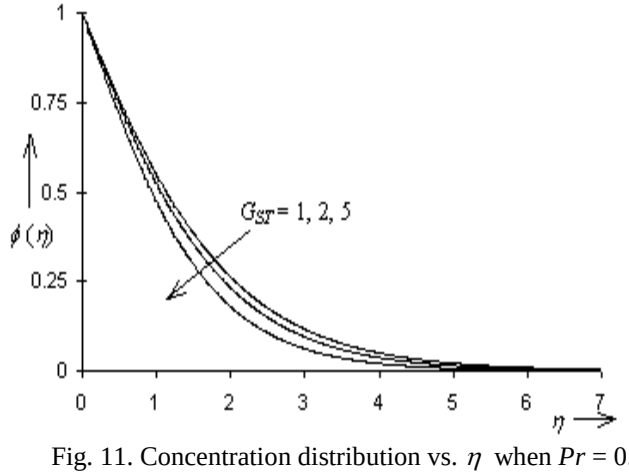

Fig. 11. Concentration distribution vs. η when Pr = 0.71, G_M = 0.5, M = 0.5, ε = 0.1, Sc = 0.5, n =1& α = 0.

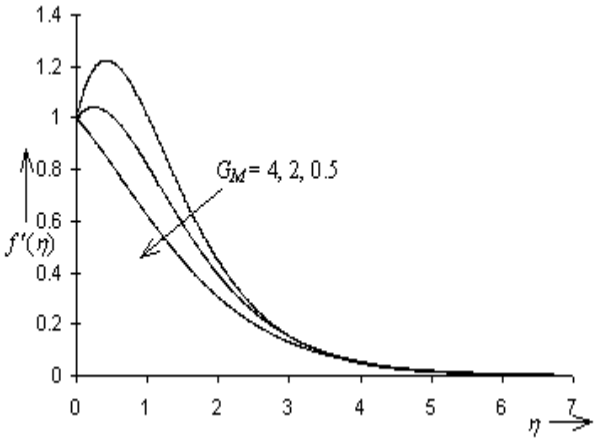

Fig. 12. Velocity distribution vs. η when Pr = 0.71, G_{ST} = 1.0, M = 0.5, ε = 0.1, Sc = 0.5, n =1 & α = 0.

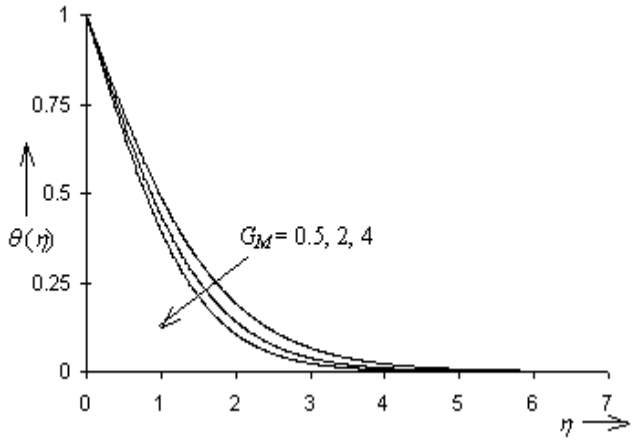

Fig. 13. Temperature distribution vs. η when Pr = 0.71, G_{ST} = 1.0, M = 0.5, ε = 0.1, Sc = 0.5, n =1 & α = 0.

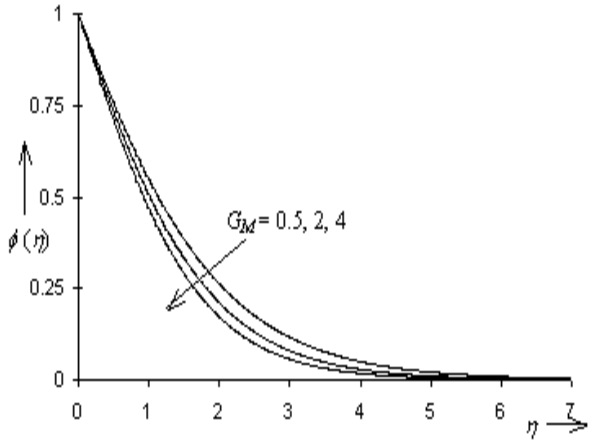

Fig. 14. Concentration distribution vs. η when Pr = 0.71, G_{ST} = 1.0, M = 0.5, ε = 0.1, Sc = 0.5, n =1 & α = 0.

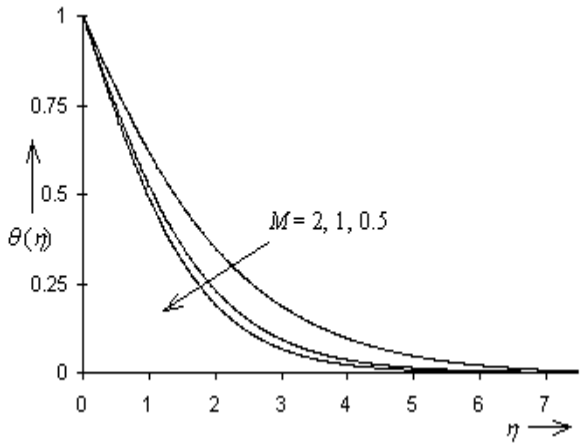

Fig. 16. Temperature distribution vs. η when Pr = 0.71, G_{ST} = 1.0, G_M = 0.5, ε = 0.1, Sc = 0.5, n =1 & α = 0.

Figures 15 to 17 depict that with the increase in magnetic parameter the fluid velocity decreases, this happens because the transverse magnetic field sets in Lorentz force, which retards the fluid velocity. The lowering of fluid velocity raises the fluid temperature and concentration, as seen from the figures 16 and 17. It is noted from figures 18 to 20 that fluid velocity and temperature decreases, while concentration of species in fluid increases with the increase in Prandtl number. Since, fluid of low Prandtl number has high thermal diffusivity hence attains higher temperature in steady state, which in turn means more buoyancy force i.e. more fluid velocity with respect to comparatively high Prandtl fluid. If fluid has high velocity, then species concentration distribution is better which is reflected as low concentration of species in the fluid. Figures 21 to 23 show that when parameter α changes from 0 to 1 the fluid velocity and fluid temperature decreases, while fluid concentration increases slightly.

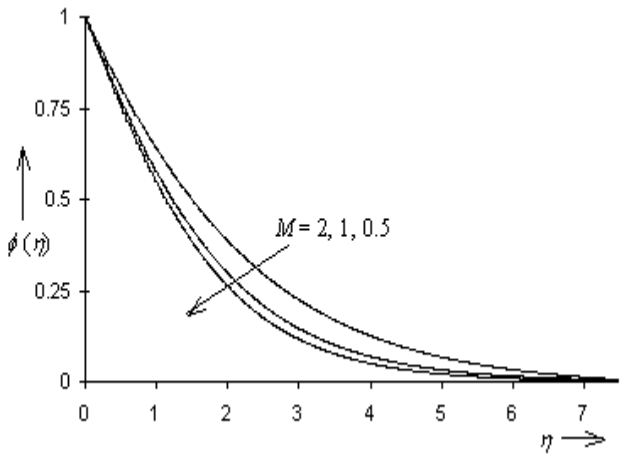

Fig. 17. Concentration distribution vs. η when Pr =0.71, G_{ST} = 1.0, G_M= 0.5, ε = 0.1, Sc = 0.5, n =1 & α = 0.

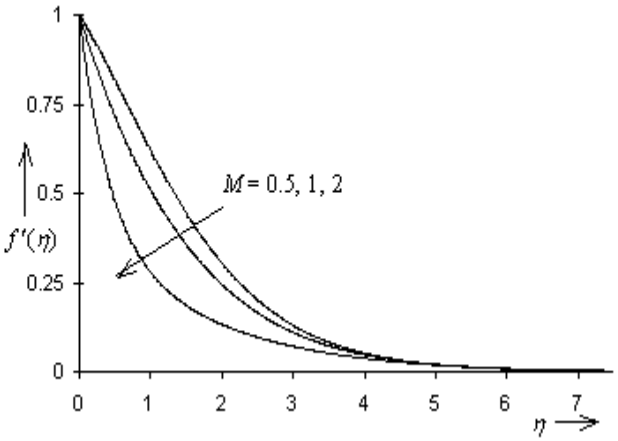

Fig. 15. Velocity distribution vs. η when Pr = 0.71, G_{ST} = 1.0, G_M = 0.5, ε = 0.1, Sc = 0.5, n =1 & α = 0.

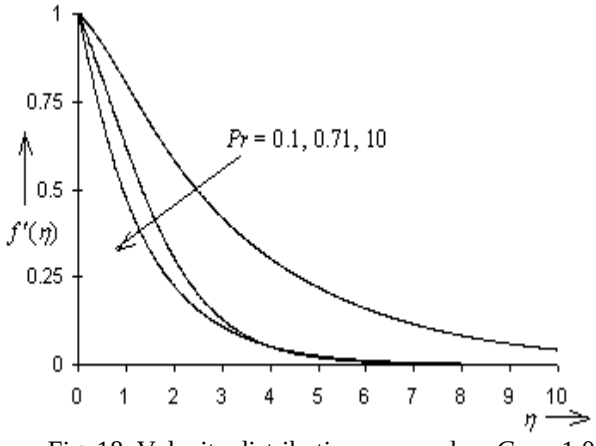

Fig. 18. Velocity distribution vs. η when G_{ST} = 1.0, G_M = 0.5, M = 0.5, ε = 0.1, Sc = 0.5, n =1 & α = 0.

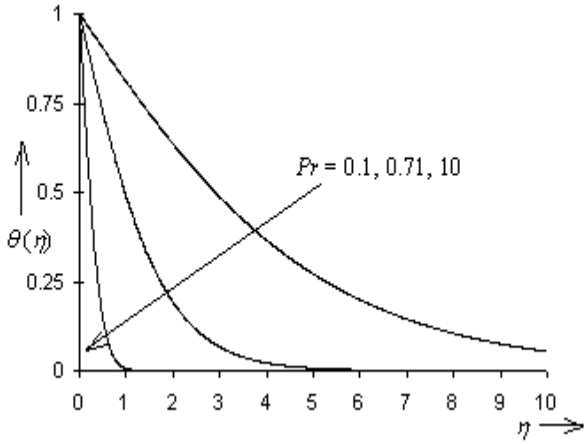

Fig. 19. Temperature distribution vs. η when G_{ST} = 1.0, G_M = 0.5, M = 0.5, ε = 0.1, Sc = 0.5, n =1 & α = 0.

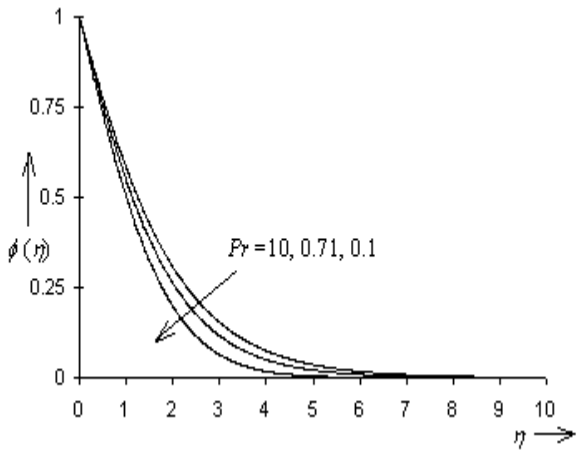

Fig. 20. Concentration distribution vs. η when G_{ST} = 1.0, G_M = 0.5, M = 0.5, ε = 0.1, Sc = 0.5, n =1 & α = 0.

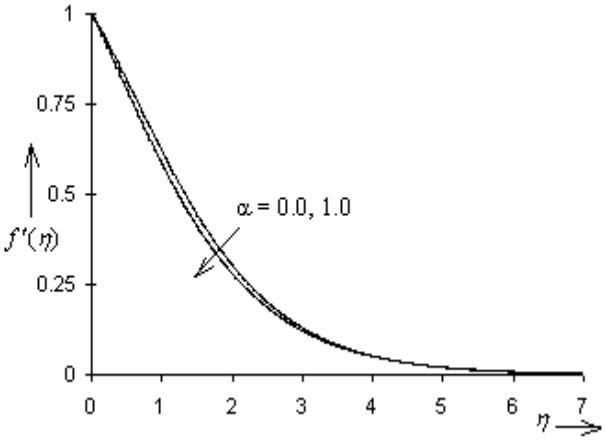

Fig. 21. Velocity distribution vs. η when Pr = 0.71, G_{ST} = 1.0, G_M = 0.5, M = 0.5, Sc = 0.5, ε = 0.1& n =1.

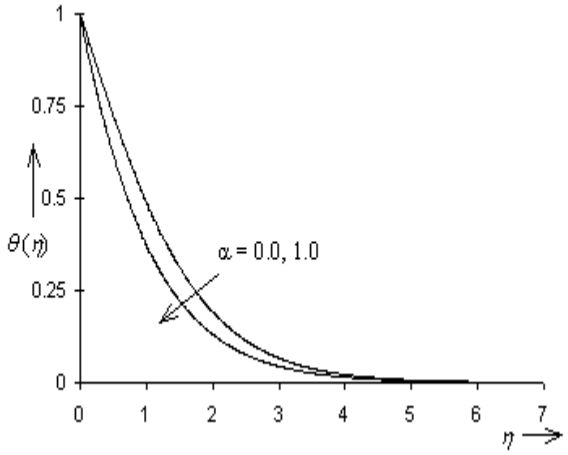

Fig .22. Temperature distribution vs. η when Pr = 0.71, G_{ST} = 1.0, G_M = 0.5, M = 0.5, Sc = 0.5, ε = 0.1& n =1.

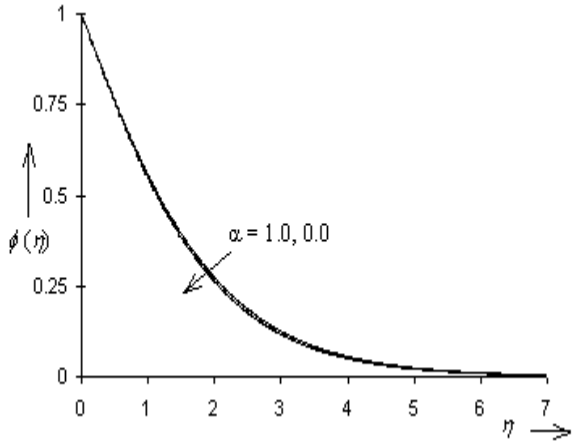

Fig. 23. Concentration distribution vs. η when Pr = 0.71, G_{ST} = 1.0, G_M = 0.5, M = 0.5, Sc = 0.5, ε = 0.1& n =1.

The fluid velocity and concentration distribution of species in PHF case is effected by the variation in different parameters in the same way as for PST, so only the temperature distribution is discussed. Figure 24 shows that with the increase in Schmidt number fluid temperature increases. This happens because fluid velocity is low at higher Schmidt number. Figure 25 depicts that fluid temperature changes negligibly with change in reaction rate parameter. It is seen from the figures 26 and 27 that at low buoyancy and modified buoyancy parameter, the fluid temperature is higher, because then the fluid velocity is comparatively lower. Figure 28 shows that with the increase in magnetic parameter the fluid temperature increases. The reason for that is the retarding force i.e. Lorentz force, which sets in presence of transverse magnetic field lowers the fluid velocity, which in turn lowers the surface cooling. Hence the surface and fluid is at higher temperature, which can also be seen in Table 5. It is noticed from figure 29 it is seen that surface and fluid temperature rises significantly as Prandtl number decreases. This phenomenon occurs because the low Prandtl fluid has high thermal diffusivity,

due to which in steady state fluid is at higher temperature thereby reducing the absorption heat from the surface and so surface attains higher temperature.

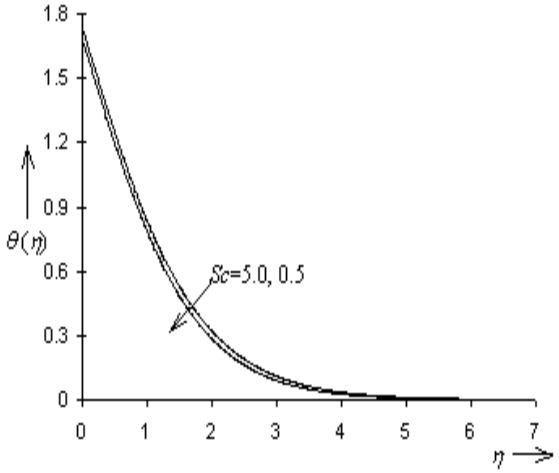

Fig. 24. Temperature distribution vs. η when Pr = 0.71, G_{HF} = 1.0, G_M = 0.5, M = 0.5, ε = 0.1 & n =1.

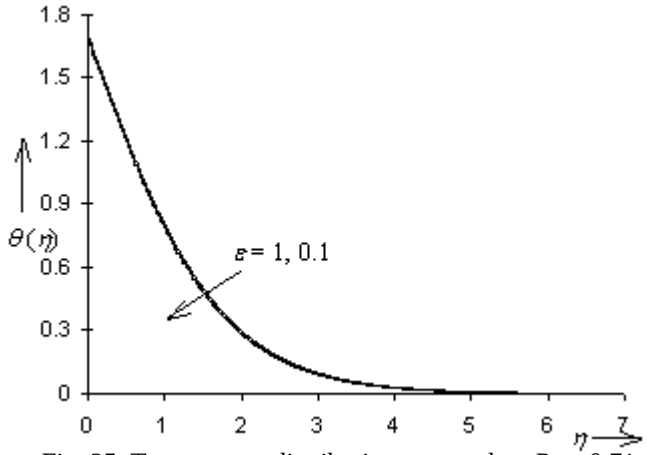

Fig. 25. Temperature distribution vs. η when Pr = 0.71, G_{HF} = 1.0, G_M = 0.5, M = 0.5, Sc = 0.5 & n =1.

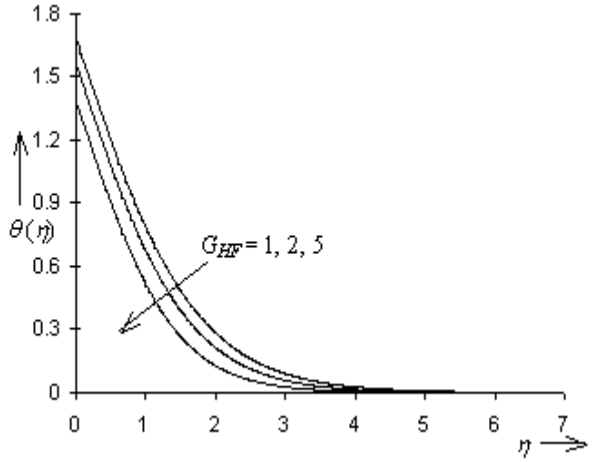

Fig. 26. Temperature distribution vs. η when Pr = 0.71, G_M = 0.5, M = 0.5, ε = 0.1, Sc = 0.5 & n =1.

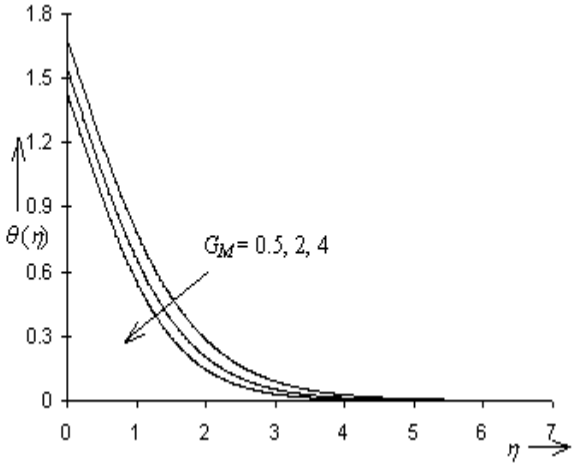

Fig. 27. Temperature distribution vs. η when Pr = 0.71, G_{HF} = 1.0, M = 0.5, ε = 0.1, Sc = 0.5 & n =1.

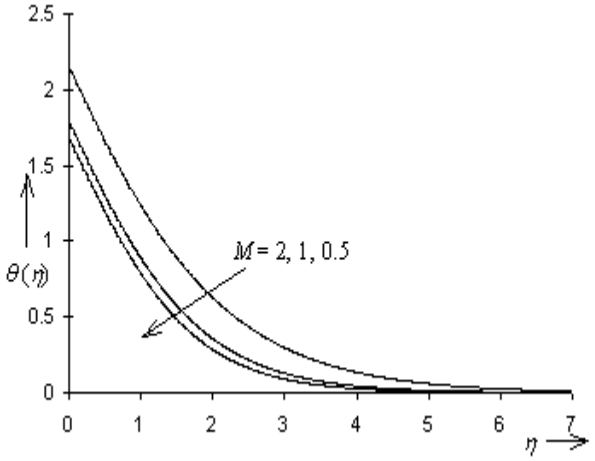

Fig. 28. Temperature distribution vs. η when Pr = 0.71, G_{HF} = 1.0, G_M = 0.5, ε = 0.1, Sc = 0.5 & n =1.

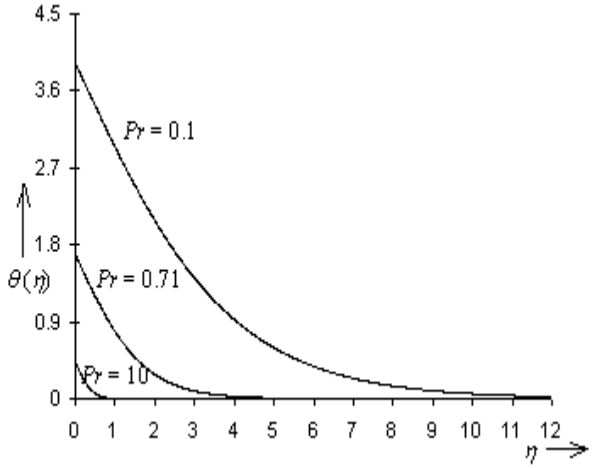

Fig. 29. Temperature distribution vs. η when G_{HF} = 1.0, G_M = 0.5, M = 0.5, ε = 0.1, Sc = 0.5 & n =1.

9. CONCLUSIONS

1. The fluid velocity and concentration of the species decrease, while fluid temperature increases with the increase in Schmidt number or reaction rate for both PST and PHF.
2. The concentration of the species in fluid increases marginally, while the fluid velocity and temperature change are negligible with the increase in order of reaction.
3. The fluid velocity increases, while the fluid temperature and concentration of the species decrease with the increase in buoyancy and modified buoyancy parameter for both PST and PHF.
4. The fluid velocity decreases, while the fluid temperature and concentration of the species increase with the increase in magnetic parameter for both PST and PHF.
5. The fluid velocity and temperature decreases, while the concentration of the species increases with the increase in Prandtl number for both PST and PHF.
6. The fluid velocity and temperature decrease, while the concentration of the species increases as α changes from 0 to 1 for PST.
7. The skin-friction coefficient decreases and the mass flux increases from surface to fluid for PST and PHF, while heat flux decreases and surface temperature increases with the increase in Schmidt for PST and PHF, respectively.
8. The mass flux at the surface reduces marginally, while the skin-friction and heat flux are practically invariant with the increase in order of reaction for both, PST and PHF.
9. The skin-friction and the mass flux at the surface increase for PST and PHF, while heat flux decreases and surface temperature increases marginally with the increase in reaction rate parameter (ε) for PST and PHF, respectively.
10. The skin-friction and the mass flux at the surface increase for PST and PHF, while the heat flux increases and surface temperature decreases with the increase in buoyancy and modified buoyancy parameters for PST and PHF, respectively.
11. The skin-friction and the mass flux at the surface decrease for PST and PHF, while the heat flux decreases and surface temperature increases with the increase in magnetic parameter for PST and PHF, respectively.
12. The skin-friction and the mass flux at the surface decrease, while the heat flux increases for PST and PHF and surface temperature decreases with the increase in Prandtl number for PST and PHF, respectively.
13. The skin-friction and the mass flux at the surface decreases for PST and PHF, while the heat flux increases and surface temperature decreases with the increase in Prandtl number for PST and PHF, respectively.
14. The skin-friction and the mass flux at the surface decrease, while the heat flux increases for PST as α changes from 0 to 1.

REFERENCES

1. P.L, Chambrė, and J.D. Young, On the diffusion of a chemically reacting species in a laminar boundary layer, *Physics of Fluids*, Vol.1, pp. 48-54, 1958.
2. B.C. Sakiadis, Boundary layer behavior on continuous solid surface- II: Boundary layer on continuous flat surface, *AIChE Journal*, Vol. 7(1), pp. 221-225, 1961.
3. L.E. Erickson, L.T. Fan and V.G. Fox, Heat and mass transfer on a moving continuous flat plate with suction or injection, *Ind. & Engg. Chem. Fund.*, Vol. 5, pp.19-25, 1966.
4. L.J. Crane, Flow past a stretching plate, *ZAMP*, Vol. 21, pp. 645-647, 1970.
5. D.T. Chin, Mass transfer to continuous moving sheet electrode, *J. Electrochem. Soc.*, Vol. 122, pp. 643-646, 1975.
6. P.S. Gupta and A.S. Gupta, Heat and mass transfer on a stretching sheet with suction or blowing, *Canadian J. Chem. Engg.*, Vol. 55(6), pp. 744-746, 1977.
7. L.J. Grubka and K.M. Bobba, Heat transfer characteristics of a continuously stretching surface with variable temperature, *Int. J. Heat Mass Transfer*, Vol. 107, pp. 248-250, 1985.
8. A. Noor, Heat transfer from a stretching sheet, *Int. J. Heat Mass Transfer*, Vol. 4, pp. 1128-1131, 1992.
9. U.N. Das, R. Deka and V.M. Soundalgekar, Effects of mass transfer on a flow past an impulsively started infinite vertical plate with constant heat flux and chemical reaction, *Forschung im Ingenieurwesen*, Vol. 60(10), pp. 284-287, 1995.
10. A.J. Chamkha, Hydromagnetic three-dimensional free convection on a vertical stretching surface with heat generation or absorption, Int. J. Heat Fluid Flow, Vol. 20, pp. 84–92, 1999.
11. A.A. Afify, MHD free convective flow and mass transfer over a stretching sheet with chemical reaction, *Heat Mass Transfer*, Vol. 40, pp. 495-500, 2004.
12. E.M. Abo-Eldahab, E.M., Hydrodymagnetic three-dimensional flow over a stretching surface with heat and mass transfer, *Heat Mass Transfer*, Vol. 41, pp. 734- 743, 2005.
13. A. Ishak, R. Nazar and I. Pop, Heat transfer over a stretching surface with variable surface heat flux in micropolar fluids, *Physics Letters A*, Vol.372, pp. 559-561, 2008.
14. A. Ishak, R. Nazar, and I. Pop, Hydromagnetic flow and heat transfer adjacent to a stretching vertical sheet, *Heat Mass Transfer*, Vo. 44, pp. 921-927, 2008.
15. A. Ishak, K. Jafar, R. Nazar and I. Pop, MHD stagnation point flow towards a stretching sheet, *Physica A*, Vol.388, pp.3377-3383, 2009.

16. A. Ishak, R. Nazar and I. Pop, Boundary layer flow and heat transfer over an unsteady stretching vertical surface, Meccanica, Vol.44, pp. 369-375, 2009.
17. A. Jeffery, Magnetohydrodynamics, Oliver and Boyed, New York, USA, 1966.
18. A. Bejan, Convective Heat Transfer, John Wiley & Sons, New York, USA, 1984.
19. A. Ishak, R. Nazar and I. Pop, Unsteady mixed convection boundary layer flow due to a stretching vertical surface, *The Arabian J Sc. Engg.*, Vol. 31(2B), pp. 167-182, 2006.
20. S.D. Conte and C. Boor, Elementary Numerical Analysis, McGraw-Hill Book Co., New York, USA, 1981.

NOMENCLATURE

g : Acceleration due to gravity of the Earth

G_{HF} : buoyancy parameter $\left\{= \dfrac{\tilde{Gr}}{\mathrm{Re}^{5/2}}\right\}$ for PHF

G_{ST} : buoyancy parameter $\left\{= \dfrac{Gr}{\mathrm{Re}^{2}}\right\}$ for PST

x, y : cartesian coordinates

C : concentration in the fluid

C_w : concentration on the sheet surface

q_w : constant heat flux

a, b : constants

D : diffusion coefficient

f : dimensionless stream function

Gr : Grashof number $\left\{= \dfrac{g\beta(T_w - T_\infty)x^3}{\nu^2}\right\}$ for PST

$\tilde{Gr}$: Grashof number $\left\{= \dfrac{g\beta(T_w - T_\infty)q_w x^4}{\kappa\nu^2}\right\}$ for PHF

B_o : magnetic field intensity

M : magnetic parameter $\left\{= \dfrac{\sigma {B_o}^2 x^2}{\mu}(\mathrm{Re})^{-1}\right\}^{1/2}$

Gr_M : modified Grashof number $\left\{= \dfrac{g\beta C_w x^3}{\nu^2}\right\}$

G_M : modified buoyancy parameter $\left\{= \dfrac{Gr_M}{\mathrm{Re}^2}\right\}$

Nu : Nusselt number

n : order of reaction

Pr : Prandtl number $\left\{= \dfrac{\mu C_p}{\kappa}\right\}$

Re : Reynolds number $\left\{= \dfrac{u_w x}{\nu}\right\}$

Sc : Schmidt number $\left\{= \dfrac{\nu}{D}\right\}$

Sh : Sherwood number

C_f : skin-friction coefficient

C_p : specific heat at constant pressure

T : temperature of fluid

T_∞ : temperature of fluid far away from sheet surface

T_w : temperature of the sheet surface

u, v : velocity components along x- and y-directions, respectively

Greek Letters

α : A constant {= 0 or 1}

β : coefficient of thermal expansion

β^* : coefficient of expansion with concentration

μ : coefficient of viscosity

κ : coefficient of thermal conductivity

ρ : density of fluid

ε :dimensionless chemical reaction parameter $\left\{= \dfrac{\lambda}{c}(C_w)^{n-1}\right\}$

ϕ : dimensionless concentration $\left\{= \dfrac{C}{C_w}\right\}$

θ : dimensionless temperature $\left\{= \dfrac{T - T_\infty}{T_w - T_\infty}\right\}$ (PST)

and $\left\{= (T - T_\infty)\left(\dfrac{q_w}{\kappa}\right)^{-1}\left(\dfrac{\nu}{c}\right)^{-1/2}\right\}$ (PHF)

σ : electrical conductivity

ν : kinematic viscosity $\left\{= \dfrac{\mu}{\rho}\right\}$

λ : reaction rate constant

η : similarity variable

ψ : stream function

Superscript

$'$: differentiation with respect to η